Nature and P-T-t constraints of very low-grade metamorphism in the Triassic-Jurassic basins, Coastal Range, central Chile

Mauricio Belmar

Diego Morata

Departamento de Geología, Universidad de Chile, Plaza Ercilla 803, Santiago, Chile
mbelmar@ing.uchile.cl
dmorata@ing.uchile.cl

ABSTRACT

Triassic-Jurassic volcano-sedimentary sequences in the Coastal Range of central Chile (34° 45/35°20'S) from the Vichuquén-Tilicura and Hualañé-Gualleco basins display metamorphic assemblages indicative of very low-grade conditions. Triassic and Lower Jurassic metapelites achieved anchizonal conditions (IC, b_o, coal-rank and fluid inclusions data: P ≈1.3, T≈190) at 181-184 Ma, under geothermal gradient of ≈35°Ckm^{-1} during extensional geodynamic conditions. Nevertheless, in stratigraphically higher mafic volcanic sequences, of Middle to Late Jurassic age, the presence of chlorite (Xc =0.98-0.99), three types of epidote (XFe^{3+} = 41.14±0.90, 30.08±1.53 and 18.05±1.75), titanite, Fe-rich and Fe-poor pumpellyite and hydrogarnet (+albite and quartz) are indicative of re-equilibration under prehnite-pumpellyite facies conditions (P ≈3 kbar, T ≈300°C) and variable oxygen fugacity. A change from an extensional setting (with maximum basin subsidence and development of burial very low-grade metamorphism in the Triassic-Lower Jurassic metapelitic sequences) to a compressional setting (with local overthrusting of Triassic and Lower Jurassic sequences over Middle to Late Jurassic volcano-sedimentary sequences) is proposed to explain the contrasting metamorphic conditions between Triassic-Lower Jurassic metapelites and Middle-Late Jurassic metabasites.

Key words: Very low-grade metamorphism, Metabasites, Triassic-Jurassic basins, Coastal Range, Central Chile.

RESUMEN

Naturaleza y estimación de las condiciones P-T-t del metamorfismo de muy bajo grado en las cuencas del Triásico-Jurásico de la Cordillera de la Costa, Chile central. Las secuencias volcano sedimentarias del Triásico-Jurásico en la Cordillera de la Costa de Chile central (34°45'/ 35° 20'S) desarrolladas en las cuencas de Vichuquén-Tilicura y Hualañé-Gualleco evidencian asociaciones metamórficas indicativas de condiciones de muy bajo grado. Las metapelitas del Triásico y Jurásico Inferior alcanzaron condiciones de anquizona (datos de IC, b_o, reflectividad de vitrinita e inclusiones fluidas: P ≈1.3, T≈190) a los 181-184 Ma, durante un contexto geodinámico extensional caracterizado por un gradiente geotérmico de ≈35°Ckm^{-1}. Sin embargo, en secuencias de rocas volcánicas máficas, estratigráficamente más altas, de edad del Jurásico Medio a Superior, la presencia de clorita (Xc =0.98-0.99), tres tipos de epidota (XFe^{3+} = 41.14±0.90, 30.08±1.53 y 18.05±1.75), titanita, pumpellyita rica en hierro y pumpellyita pobre en hierro e hidrogranate (+ albita y cuarzo) es indicativa de un ajuste en el equilibrio metamórfico en las condiciones de la facies prehnita pumpellyita (P ≈3 kbar, T ≈300°C) y bajo variaciones importantes en la fugacidad de oxigeno. Se propone un cambio en el contexto geodinámico desde un ambiente extensional (en el que se alcanzaría la máxima subsidencia y se desarrollaría el metamorfismo de tipo 'burial' en las secuencias metapelíticas del Triásico- Jurásico Inferior) a un ambiente contraccional, en el que la superposición local de las secuencias del Triásico y Jurásico Inferior sobre las del Jurásico Medio-Superior permitiría alcanzar las condiciones P-T calculadas y, de este modo, justificar las diferencias encontradas entre las condiciones metamórficas de las metapelitas del Triásico-Jurásico inferior y las de las metabasitas del Jurásico Medio-Superior.

Palabras claves: Metamorfismo de muy bajo grado, Metabasitas, Cuencas triásico jurásicas, Cordillera de la Costa, Chile central.

Revista Geológica de Chile, Vol. 32, No. 2, p. 189-205, 6 Figs. 6 tables, July 2005.

INTRODUCTION

Recent progress on very low-grade metamorphic studies were summarized by Frey and Robinson (1999). For low-grade metapelites, much emphasis has been given in measuring reaction progress (*e.g.,* Merriman and Peacor, 1999) and determining contrasting geotectonic settings (Merriman and Frey, 1999). Numerical maturity models calibrated by vitrinite reflectance data has been demonstrated to be very useful in determining the thermal history during very low-grade metamorphism (*e.g.,* England and Bustin, 1985; Langenberg and Kalkreuth, 1991; Ferreiro Mählmann, 2001). Also, comparison of vitrinite reflectance with clay mineral data can be used as a first approximation of the duration of metamorphism and the thermo-tectonic history (*e.g.,* Bevins *et al.*, 1996; Ferreiro Mählmann, 2001).

In addition, illitic clay minerals have been used in several studies to constrain the timing of very low- and low-grade events. In fact, authigenic illite and mixed illite-smectite have been shown to be reliable 'clocks' at temperatures below 260± 20ºC (Hunziker *et al.*, 1986), a property that makes them potentially attractive tools for reconstructing the burial history.

In the central Andes of Chile, near Santiago, very low-grade metamorphism of mafic rocks ranging from zeolite to upper greenschist facies is widespread and has been studied in some detail (Aguirre *et al.*, 1978, 1997, 1999, 2000; Bevins *et al.*, 2003; Levi, 1969; Levi *et al.*, 1982; Robinson *et al.*, 2004; Vergara *et al.*, 1993). However, little is known about low-grade metamorphism in the sedimentary rocks in central Coastal Chile (Ruiz Cruz *et al.*, 2002, 2004).

Belmar *et al.* (2002) determined the P-T conditions of the Triassic-Jurassic basins south of Santiago, by applying the techniques of illite crystallinity (IC), coal rank determination, fluid inclusion microthermobarometry, identification of index minerals and critical mineral assemblages and thermal maturity modelling. Values of T~190°C and P~1.3 kbar were obtained. Belmar *et al.* (2002, 2004) distinguished between regional burial low-grade metamorphic events and local contact metamorphism related to the thermal influence of plutonic intrusions in the Triassic-Jurassic basins. These distinctions are relevant, because the occurrence of intrusions are common in the history of the Andean evolution, with subsidence and magmatic events since Palaeozoic to the present time. Finally, by dating of whole rock and <2 μm size fraction of these Triassic-Jurassic metapelites, Belmar *et al.* (2004) constrained the geochronology of the diagenesis (206 Ma), the anchizonal very low-grade metamorphism (181-184 Ma) and a late hydrothermal event (155 Ma).

In this study, therefore, the authors aim to distinguish between very low-grade metamorphism in sedimentary rocks, and that present in volcanic mafic rocks of Middle-Late Jurassic age. For this purpose, the well known Hualañé-Gualleco Triassic-Jurassic volcano-sedimentary basins in the Coastal Range of central Chile represent an excellent opportunity to assess metamorphic paragenesis developed in andesitic lava flows, and those developed in the underlying metasedimentary rocks of Triassic-Jurassic age, previously studied by Belmar *et al.* (2002, 2004). In this work, mineral chemistry of metabasites will be used to establish the new P-T metamorphic conditions of this basin. The significance of this very low-grade metamorphism will be then discussed on the basis of its geologic context.

GEOLOGICAL SETTING

The study area is located in the Coastal Range of central Chile between 34º45' and 35°20'S, *ca.* 300 km southwest of Santiago (Fig. 1). Late Triassic to Early Jurassic marine to continental sedimentary rocks and Middle to Late Jurassic volcanic rocks are exposed in the region. The sedimentary rocks form part of an almost continuous belt, approximately 60 km long and unconformably overlying a Late Paleozoic metamorphic basement (Fig. 1). Tectonic development during Triassic times was controlled

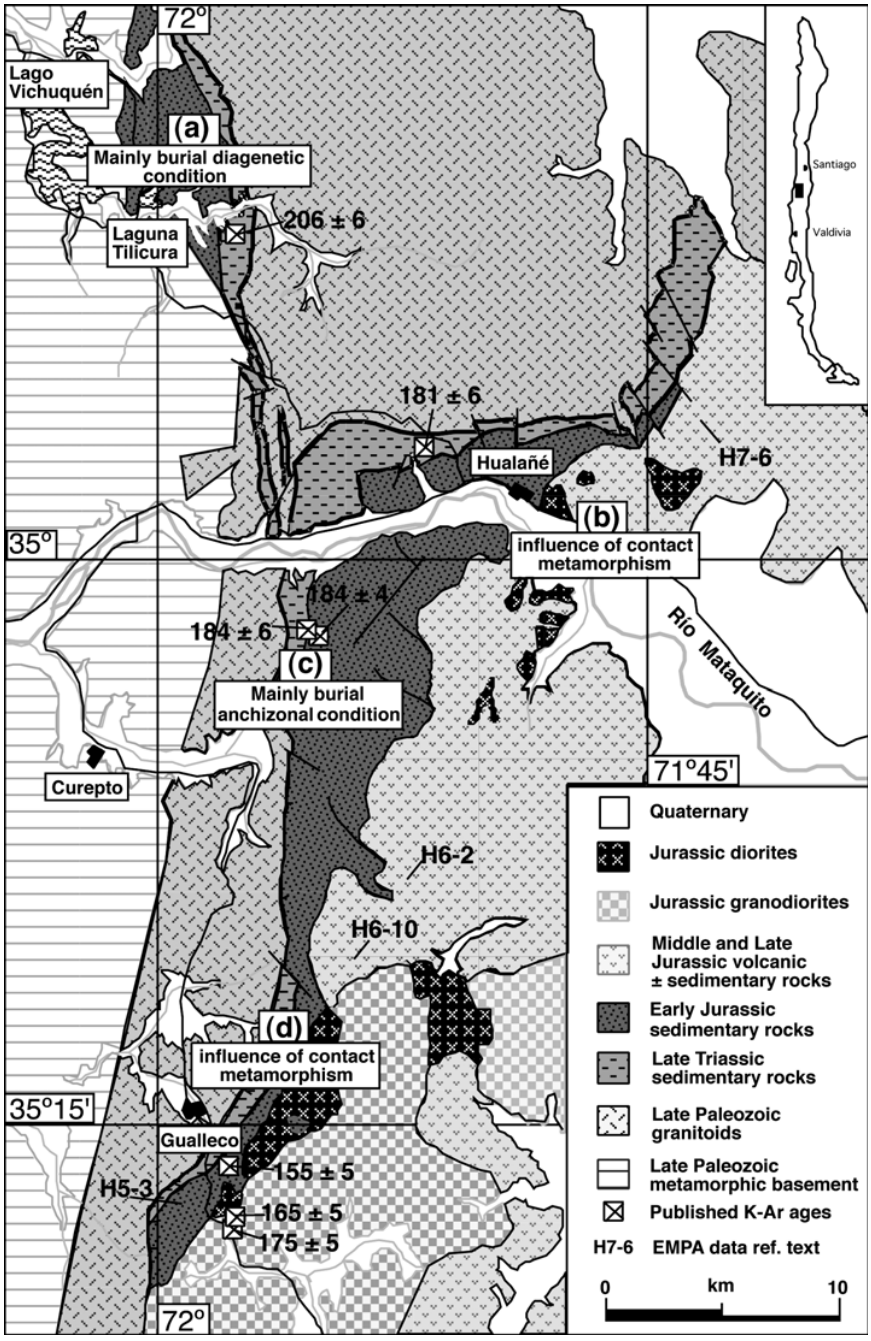

FIG. 1. Simplified geological map (modified from J. Corvalán[1] and Belmar *et al.,* 2002) of the Triassic-Jurassic formations of the Coastal Range in central Chile at 34°45' to 35°20'S, with the Vichuquén-Tilicura basin in the north and the Hualañé-Gualleco basin in the south; location of the analyzed samples used in this work is shown. Areas (a), (b), (c) and (d) after Belmar *et al.* (2004) and referred to in table 1.

[1]1994. El Triásico y Jurásico de Vichuquén, Hualañé, Curepto y Gualleco (Unpublished), *Servicio Nacional de Geología y Minería.*

by continuous movements and differential uplift of the Paleozoic basement until, at least, the Jurassic (Thiele and Morel, 1981). The western Palaeozoic areas were exhumed faster than the eastern area, on which Mesozoic sedimentary rocks were preserved (Thiele and Morel, 1981). Uplift of the western Paleozoic basement during the Late Triassic and Early Jurassic was concomitant with the development of two sedimentary basins, the Vichuquén-Tilicura basin to the north and the Hualañé-Gualleco basin further to the southeast (Fig. 1). In the northern Vichuquén-Tilicura basin the late Triassic sedimentary rocks are characterized by a marine sequence of shales, sandstones and conglomerates (J. Corvalán[1]). The eastern border of the Vichuquén-Tilicura basin (Fig. 1) and the basement of the Hualañé-Gualleco basin is represented by Carboniferous granitoids (Munizaga *et al.*, 1973). West of the Vichuquén-Tilicura basin (Fig. 1) a late Palaeozoic metamorphic basement is exposed (González Bonorino and Aguirre, 1970; Munizaga *et al.*, 1973; Hervé *et al.*, 1982), generally interpreted as a transition from weakly deformed retro-wedge sediments exposed to the east (Eastern series) to an accretionary complex in the west (Western Series) (Hervé, 1988; Martin *et al.*, 1999; Willner *et al.*, 2000).

The Hualañé-Gualleco basin (J. Corvalán)[1] is located between the two homonymous villages (Fig. 1). The Late Triassic to Early Jurassic sequence of mainly sedimentary rocks reaches a maximum thickness of 2600 m at the east of the village of Curepto (Fig. 1). The outcrops are located at both banks of the Mataquito River. The lowest 500 m of the stratigraphic pile corresponds to the Late Triassic unit and comprises predominantly shales with quartzitic sandstones, conglomerates, subarkoses and subgraywackes. The Hualañé-Gualleco basin was intruded by Jurassic diorites and granodiorites, at 165 ± 5 Ma (K-Ar on biotite) to 175±5 Ma (K-Ar on hornblende) (Gana and Hervé, 1983). Most of the eastern part of the study area is composed of andesitic lava flows, volcanic breccias and minor marine sedimentary intercalations of Middle and Late Jurassic age (Fig. 1), which read a maximum thickness of *ca*. 3,600 m and belong to the Altos de Hualmapu Formation (Morel, 1981; Bravo, 2001). No isotopic data are available for this unit, but marine paleontological fauna present in sedimentary rocks, assigned to the Toarcian, indicates the end of the marine sedimentation (Corvalán, 1982) . In the southern part of the area, the volcanic units are also intruded by Jurassic diorites and granodiorites similar to those described above (Fig. 1). For a detailed stratigraphic description, columns, profiles and paleontological determination see Belmar *et al.* (2002).

PREVIOUS WORK ON THE VERY LOW-GRADE METAMORPHISM OF THIS AREA

Diagenetic to very low-grade metamorphic P-T conditions have been determined for Late Triassic to Early Jurassic sedimentary rocks from the Vichuquén-Tilicura and the Hualañé-Gualleco basins in central Chile using illite crystallinity Kübler Index (KI, Kübler 1967, 1984), coal rank data, K-white mica b cell dimension (Sassi and Scolari, 1974), characteristic mineral assemblages and fluid inclusion data (Belmar *et al.*, 2002). A burial-related diagenetic to low-grade metamorphic event, recorded in both basins, is locally overprinted in the Hualañé-Gualleco basin by contact metamorphism around the Jurassic dioritic to granodioritic intrusions (Fig. 1). Diagenetic conditions prevailed in the northern Vichuquén-Tilicura basin, whereas in the southern Hualañé-Gualleco basin low-grade metamorphism is observed with an increase in metamorphic grade from north to south. Epizonal conditions are locally reached south of the Hualañé-Gualleco basin. Low-pressure conditions were determined by Belmar *et al.* (2002) using the geobarometer of the b cell dimension of K-white mica. A time-interval of *ca.* 20 Ma between diagenesis (206±6 Ma) and anchizonal very low-grade metamorphism (181±6 - 184±4 Ma, K-Ar ages on the <2µm grain size fractions of shales) was recorded by Belmar *et al.* (2004). A subsidence rate of *ca*. 120 m/Ma was proposed for these

Triassic-Jurassic basins, and a thermal influence on this very low-grade burial regional metamorphism was invoked (Belmar *et al.*, 2004).

Contact metamorphic field relationships between Jurassic intrusions and Jurassic sedimentary rocks are only visible in fresh roadcuts, only few meters away from intrusions near Gualleco. A hornfels facies assemblage with quartz, plagioclase, flakes of biotite with inclusions of Ti-Fe-phases and anhedral ferrosilite was characterized by electron microprobe analyses (Belmar *et al.*, 2002).

ANALYTICAL METHODS

Previous work on *ca.* 100 samples including shales, slates of Late Triassic to Late Jurassic age, carried out by Belmar *et al.* (2002), was presented above. The present work comprises additional sampling and studies principally on metabasites of Middle to Late Jurassic age allowing a new interpretation of P-T-t conditions.

Chemical analyses and scanning electron microscope (SEM) images of minerals were obtained using a JEOL JXA-8600 Superprobe at the University of Basel (Switzerland). Olivine (Mg, Fe, Si), orthoclase (K, Al), synthetic graftonite (Mn), albite (Na) and wollastonite (Ca) were used as standards. All elements were measured using wavelength dispersive spectrometry, an accelerating voltage of 15 kV and a beam current of 10 nA. In general, counting times for major and minor elements were 10 s and 20 s, respectively and the background counting time was set to 5 σ. The beam was focused to a spot size of 2 μm. Data were reduced using the PROZA correction program for all silicates, except data from pumpellyite and epidote, on which the program ZAF (due to the high Fe-content) was used.

RESULTS

METAPELITES

Results from various analytical methods are presented by Belmar *et al.* (2002) and summarized here in table 1. The Coal Rank values (R_{max}) vary in a similar manner to the Kubler Index (KI) data, showing a good correlation between each other, with a general increase southward with considerable scatter in the data. The highest coal rank of the meta-anthracite stage is found in the vicinity of granodioritic-dioritic intrusions.

In the northern part of the Hualañé-Gualleco basin, coal rank values increase from west to east. Samples with values >6% R_{max} have textures of natural coke and pyrolitic carbon, which is formed after chemical cracking of volatiles. The pyrolitic carbon forms spherical fibrolitic bodies (<50 μm) with helicitic extinction (anisotropic fibroblastic structure showing Brewster cross) and display optical features of a short and fast thermal overprint, as described by Ferreiro Mählmann (2001). As in the southern part of the Hualañé-Gualleco basin, the highest coal rank is also associated with textures of pyrolitic carbon.

METABASITES

In the upper part of the Jurassic unit, southeast of the Río Mataquito, the sedimentary rocks are increasingly interbedded with the Middle to Late Jurassic porphyritic andesitic lavas and breccias from the Altos de Hualmapu Formation (Morel, 1981). They contain euhedral plagioclase and augite as the main phenocrysts set in a cryptocrystalline to microcrystalline groundmass. Chlorite and calcite are the main alteration minerals and plagioclase is partly to completely albitized ($An_{0.4\text{-}21}Or_{0.4\text{-}0.5}$ but mostly from $An_{0.4}Or_{0.4}$ to $An_8Or_{0.4}$).

Chlorite is the most common metamorphic mineral, mostly replacement patches inside plagioclase and clinopyroxene phenocrysts, as inclusions in vugs and also as interstitial material in the groundmass. Most chlorite is pale-green, although yellowish- green pleochroic types appear with

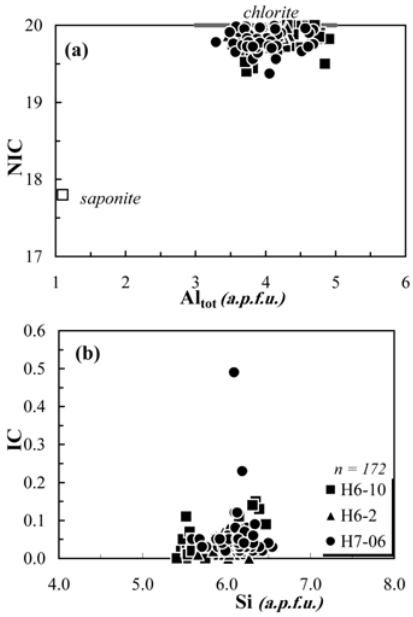

FIG. 2. Mafic phyllosilicate compositions from the Middle and Late Jurassic volcanic rocks of the Hualañé-Gualleco basin; (**a**) non-interlayer cations (NIC = Si+Al+Fe+Mg+Mn+Ti a.p.f.u.) *versus* total Al (a.p.f.u.). Different symbols represent analyses from different samples (see location of analysed samples on Fig. 1). Ideal end-member of saponite, shown by open squares, and chlorite solid solution compositional range from Schiffman and Friedleifsson (1991) and slightly modified by Robinson *et al*. (1993); (**b**) interlayer cations (IC = Ca+Na+K, a.p.f.u.) *versus* Si (a.p.f.u.). Data with IC<0.2 and Si ≈6.0 can be considered as chlorite without smectite layers.

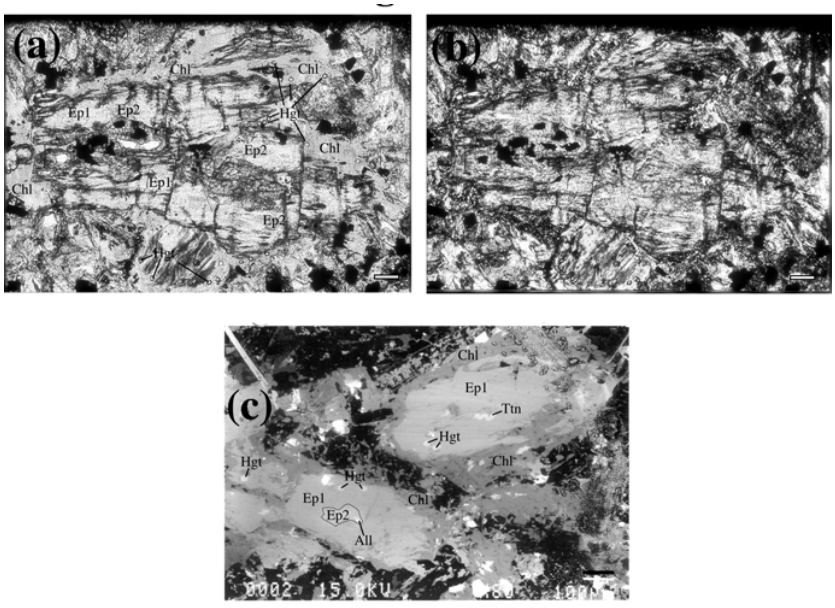

FIG. 3. Microphotographs of two types of epidote (iron-poor Ep1 and iron-rich Ep2) coexisting with chlorite (Chl) and small crystals of hydrogarnet (Hgt) from Middle-Late Jurassic volcanic rocks of the Hualañé-Gualleco basin (sample H7-10). (a) = plane light; (b) crossed polars. Scale bar = 0.2 mm. (c) Back-scattered electron image of sample H7-10 showing small allanite crystals (All) overgrow by Ep2 and Ep1. Small idiomorphic hydrogarnet (Hgt) and irregular titanite (Ttn) are also present. Scale bar =100 μm.

TABLE 1. SUMMARY OF METAPELITES VERY LOW-GRADE METAMORPHISM IN THE TRIASSIC-JURASSIC METAPELITES FROM THE VICHUQUÉN-GUALLECO BASINS, COASTAL RANGE, CENTRAL CHILE.

Basin	Vichuquén-Tilicura	Hualañé-Gualleco		
sub-zone		Center	East	South
area of figure 1	(a)	(c)	(b)	(d)
Kubler Index				
Range (Δ°2Q)	0.20 to 0.40	0.43 to 0.52	0.46 to 0.31	0.29 to 0.5
stage	High diagenetic zone	Low anchizone	Anchizone/ diagenesis	Epizone/ anchizone
Coal rank				
Rmax %	2.8 to 3.1	2.9 to 4.1	5.5 to 7.5	4.9 to 6.5
stage	Anthracite	Meta-anthracite	High meta-anthracite	High meta-anthracite
Fluid inclusion				
Temperature in °C	-	179± 4 ; 190± 10	223± 12	-
Pressure in Kbar	-	1.4 ; 1.3	1,3	-
Mineral index				
XRD	Illite/smectite	Pyrophyllite-paragonite	Paragonite	Hornfels facies
Illite/smectite ordering				
% Illite	65 to 85 %	85 to 90 %	100%	100%
Temperature in °C	170 to 190	150 to 230	-	-
Pressure in Kbar		< 1.5	-	-
K-Ar (Ma) date sediments				
<2µm size fraction	206±6	181±6;184±4;184±6	-	155±5
whole rock	395±12	221±7;559±16;219±7	-	174±5
K-Ar (Ma) date Intrusion				
Biotite		-	-	165±5
Hornblende		-	-	175±5
Contact metamorphism				
Temperature in °C		-	-	655 to 691
Pressure in Kbar		-	-	<4

anomalously deep blue to brownish grey interference colours. Microprobe analyses of chlorite (Table 2a) were normalized to 28 oxygens and fulfill the criterion (Na+Ca+K) a.p.f.u.< 0.20 as a constraint for microprobe analyses uncontaminated by other phases (Schmidt *et al.*, 1997). Projection of chlorite composition on the Al_{total} *versus* non-interlayer cations (NIC) diagram (Fig. 2a) indicates a rather homogenous composition in all analysed samples, close to the clinochlore end-member. X_c values (proportion of chlorite layers in mixed-layer chlorite/smectite calculated from microprobe analyses after the Wise method, in Bettison and Schiffman, 1988) range from 0.98 - 0.99; low Σ (Na+K+Ca) a.p.f.u. values (<0.2, Fig. 2b) is consistent with the very low contents of interlayered smectite.

Epidote occurs frequently in the lava flows; it is associated with chlorite, titanite, magnetite, calcite and, locally, pumpellyite and hydrogarnet. Epidote replaces plagioclase and clinopyroxene phenocrysts along fissures, and it is also observed (in minor amounts) as small crystals in the groundmass and (preferentially) filling the cores of vugs and interstices. Three types of epidote are distinguished in the sampling area (Table 2b): (1) brownish variety with a pistacite (XFe^{3+}) contents from 39.7 to 42.7; (2) yellow variety, that always occurs inside the brownish one (Figs. 3, 4a), having XFe^{3+} values of 26.6-32.9 and (3) is of yellow pale green colour with XFe^{3+} = 15.4 to 21.1. In addition another type of epidote, characterised by the presence of Ce, Nd and La, suggesting an allanitic component, was occasionally detected.

Titanite occurs as dusty granules or small spherical aggregates at the rim of vugs and interstices associated with chlorite, epidote (Fig. 3c) as well as dispersed spots in the groundmass. Al_2O_3 contents range between 2.0-4.8 wt% and Fe_2O_3 between 1.4-7.8 wt% (Table 2c). These values are similar to those of titanites developed in prehnite-

TABLE 2a. CHLORITE ANALYSES, STOICHIOMETRY CALCULATED ON THE BASIS OF 28 OXIGENS.

Sample	H6-10 Mean n=60	St. dev.	H6-2 Mean n=45	St. dev.	H7-6 Mean n=67	St. dev.	H5-3 Mean n=14	St. dev.
SiO_2	27.09	1.70	27.65	0.80	28.82	1.35	25.95	0.96
TiO_2	0.07	0.19	0.05	0.05	0.03	0.05	0.24	0.27
Al_2O_3	17.66	1.27	15.68	0.86	15.86	1.20	17.09	0.84
FeO	23.04	1.60	29.66	1.02	25.15	1.39	31.22	2.37
MnO	0.64	0.42	0.66	0.09	0.45	0.10	0.61	0.20
MgO	17.26	0.55	13.08	0.53	16.02	1.16	9.75	1.97
CaO	0.11	0.12	0.08	0.05	0.19	0.27	0.18	0.26
Na_2O	0.01	0.01	0.02	0.02	0.02	0.02	0.03	0.05
K_2O	0.03	0.04	0.03	0.03	0.02	0.02	0.15	0.20
Total	**85.92**	**1.92**	**86.91**	**1.15**	**86.55**	**1.72**	**85.22**	**0.88**
Si	5.78	0.16	6.04	0.11	6.15	0.16	5.86	0.13
Ti	0.01	0.03	0.01	0.01	0.01	0.01	0.04	0.04
Al total	4.44	0.39	4.05	0.22	3.99	0.31	4.55	0.25
Al(iv)	2.22	0.16	2.09	0.11	2.14	0.16	2.41	0.13
Al(vi)	2.22	0.23	1.96	0.12	1.85	0.17	2.14	0.18
Fe^{+2}	4.11	0.35	5.42	0.24	4.49	0.32	5.90	0.55
Mn	0.12	0.07	0.12	0.02	0.08	0.02	0.12	0.04
Mg	5.49	0.31	4.26	0.17	5.10	0.36	3.28	0.61
Ca	0.03	0.03	0.02	0.01	0.04	0.06	0.04	0.06
Na	0.00	0.01	0.01	0.01	0.01	0.01	0.01	0.02
K	0.01	0.01	0.01	0.01	0.00	0.01	0.04	0.05
Xc	0.98	0.11	0.94	0.05	0.89	0.07	-	-
T°C	296	25	253	23	237	20	-	-
NIC	19.84	0.67	19.65	0.30	19.34	0.40	-	-
IC	0.04	0.03	0.03	0.02	0.05	0.06		

Notes: T°C Cathelineau (1988); **NIC =** Si+Al+Fe+Mg+Mn; **IC =** Na+K+Ca;**Xc =** Proportion of Chl in Chl/Smc; all Fe assumed to be Fe^{2+}; **n= 60=** number of analyses; **St dev=** standard deviation; **H5-03** chlorite from retrograde in hornfels facies, no sence temperature calculation.

pumpellyite facies terranes in central Sweden (Nyström, 1983) and in the meta-andesites of the Celica Formation in southwestern Ecuador (Aguirre, 1992).

Pumpellyite is present in only one of the studied sample from the northeasternmost part of the Hualañé-Gualleco basin (sample H7-06, Fig. 1). Pumpellyite is associated with hydrogarnet-epidote-chlorite-titanite-calcite-magnetite; this assemblage is reported for the first time in this area. Although optically homogeneous, two intergrown pumpellyite types can be distinguished chemically (Table 2d and Figs. 4a, 4b). Pumpellyite of type 1 has FeO* contents between 9.25 and 11.75 wt% and Al_2O_3 contents between 19.69 and 21.64 wt%. Pumpellyite of type 2 has lower FeO* values, ranging between 5.56-8.8 wt%, and Al_2O_3 values ranging between 21.24 and 23.03 wt% (Fig. 4a, b).

Hydrogarnet from the same thin section (H7-06) occurs as framboidal grains with a diameter of up to 20 µm within chlorite patches of the groundmass and also in chlorite-epidote vugs (Fig. 3). Hydrogarnet analyses (And_{57} - Gro_{43}, XFe^{3+} values ranging from 53.3 to 62.7%, and low MgO (max. 0.36 wt% contents) have low totals (between 95 and 99 wt%, Table 2e), a feature which shared by framboidal grandites and attributed by Coombs *et al.* (1977) to fluid-filled microcavities.

TABLE 2b. EPIDOTE ANALYSES, BASED ON 12.5 OXYGENS.

	Type 1 Mean n=15	Type 2 St. dev.	Type 3 Max. value	Min. value	Mean n=45	St. dev.	Max. value	Min. value	Mean n=13	St. dev.	Max. value	Min. value
SiO_3	36.49	0.34	36.82	35.76	37.28	0.87	38.91	35.09	37.78	1.15	39.52	36.28
TiO_2	0.08	0.06	0.21	0.00	0.12	0.18	0.59	0.00	0.04	0.05	0.12	0.00
Al_2O_3	17.87	0.36	18.39	17.00	21.89	0.71	23.74	20.30	25.64	1.05	27.27	24.23
Fe_2O_3	19.56	0.51	20.60	18.86	14.75	0.89	16.21	12.67	8.85	0.94	10.28	7.52
MnO	0.09	0.06	0.18	0.00	0.18	0.15	0.77	0.00	0.13	0.13	0.48	0.00
MgO	0.05	0.03	0.15	0.02	0.12	0.16	0.67	0.00	0.01	0.02	0.08	0.00
CaO	22.19	0.50	23.18	21.13	22.35	0.42	23.15	21.52	22.97	0.36	23.54	22.05
Na_2O	0.02	0.03	0.10	0.00	0.01	0.01	0.05	0.00	0.01	0.01	0.04	0.00
K_2O	0.01	0.01	0.02	0.00	0.01	0.01	0.03	0.00	0.01	0.01	0.03	0.00
Total	**96.35**	**1.10**	**97.55**	**92.93**	**96.72**	**1.88**	**100.86**	**92.19**	**95.44**	**2.50**	**99.47**	**92.55**
Si	3.03	-	-	-	3.02	-	-	-	3.03	-	-	-
Al (iv)	0.00	-	-	-	0.00	-	-	-	0.00	-	-	-
Al (vi)	1.75	-	-	-	2.09	-	-	-	2.42	-	-	-
Ti	0.00	-	-	-	0.01	-	-	-	0.00	-	-	-
Fe^{3+}	1.22	-	-	-	0.90	-	-	-	0.53	-	-	-
Mn	0.01	-	-	-	0.01	-	-	-	0.01	-	-	-
Mg	0.01	-	-	-	0.01	-	-	-	0.00	-	-	-
Ca	1.97	-	-	-	1.94	-	-	-	1.98	-	-	-
Na	0.00	-	-	-	0.00	-	-	-	0.00	-	-	-
K	0.00	-	-	-	0.00	-	-	-	0.00	-	-	-
XFe^{3+}	41.14	0.90	42.67	39.67	30.08	1.53	32.90	26.57	18.05	1.75	21.12	15.40

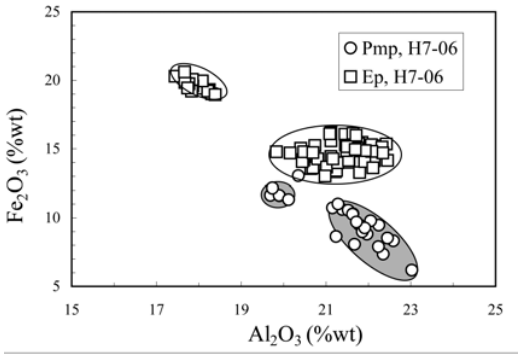

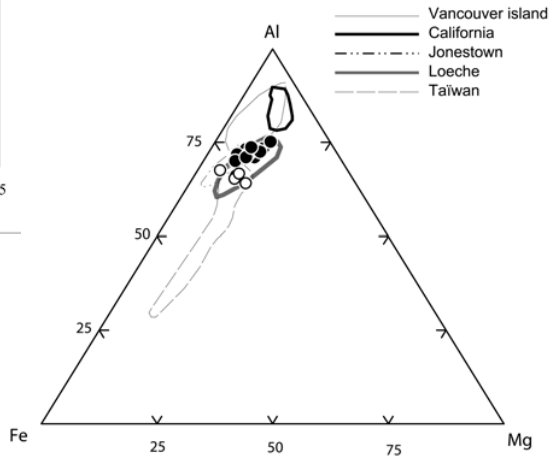

FIG. 4. Compositional diagrams for epidote and pumpellyite in sample H7-06. (a) Al_2O_3 (wt%) *versus* Fe_2O_3 (wt%) for epidote (white squares) and pumpellyite (white circles) showing the high- and low-iron groups. (**b**) Al: Fe:Mg diagram (Coombs *et al.*, 1979) for pumpellyite. Circles in white: iron rich pumpellyite; circles in black: iron poor pumpellyite. Reference fields taken from Coombs *et al.* (1979) and Liou and Ernst (1979).

DISCUSSION

P-T CONDITIONS OF VLGM IN METAPELITES

In table 1 the main parameters for determination of metamorphic grade and P-T- t conditions are summarized from Belmar *et al.* (2002, 2004). In the study area, the maturation of organic matter (coalification) and Kübler index increase simultaneously up to anchizonal conditions representing the low-grade metamorphic burial event. Nevertheless, certain samples violate this general trend. The highest vitrinite reflectance values are due to a high temperature heating event caused by the local emplacement of intrusions nearby, because of the highest sensitivity of the maturation of organic matter to temperatures with respect to the KI (Belmar *et al.*, 2002).

The mineral index identified using XRD (Belmar *et al.*, 2002) are characteristic for each metamorphic zone. Thus, sedimentary rocks with illite/smectite are located in the high diagenetic zone; paragonite is present from the beginning of the anchizone to the lower epizone; and pyrophyllite appears in the anchizone.

The interpretation of fluid inclusion data (Belmar *et al.*, 2002) indicates that this very low-grade metamorphism was formed during a burial-induced heating event at $T \leq 190°C$ and $P \leq 1.3$ kbar. Assuming $P_{fluid} = P_{total}$, an overburden of *ca*. 4.8 km can be deduced (rock density ≈2.7) and the prevailing geothermal gradient was calculated to be >35°C/km. These low-pressure conditions are consistent with b_o measurements carried out in illites from associated metapelites (Belmar *et al.*, 2002) (Fig. 5).

P-T CONDITIONS OF VLGM IN METABASITES

Pumpellyite is one of the most representative mineral index of very low-grade metamorphism in metabasites; its coexistence with other calc-aluminium silicate (epidote, actinolite and/or prehnite), together with chlorite and quartz, define different metamorphic facies in a P-T space (Frey *et al.*, 1991). Systematic analyses of pumpellyites has established a qualitative relationship between pumpellyite composition (mostly in relation with the $Al \Leftrightarrow Fe^{3+}$ substitution) and P-T conditions during low-grade metamorphism (see Beiersdorfer and

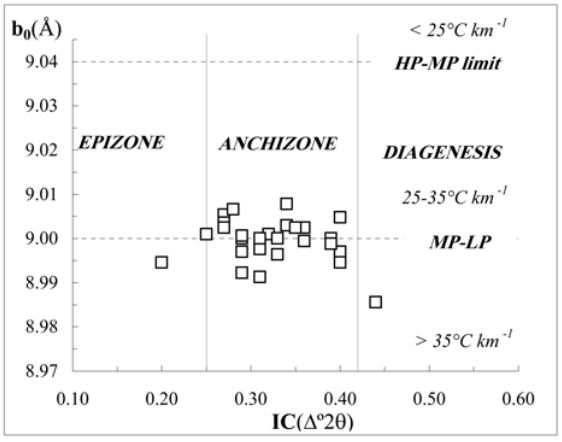

FIG. 5. Illite crystallinity - Kübler index (IC) *versus* b_0 data of illites from metapelites from the Triassic-Jurassic sequences in the Vichuquén basin. HP, MP and LP = high, middle and low pressure and inferred geothermal gradient according to the b_0 data (Guidotti and Sassi, 1986). IC and b_0 data from Belmar *et al.* (2002).

Day, 1995 for a review). Iron-rich pumpellyites with variable Al-content are relatively common in the lowest grade assemblages and seem to be characteristic of low metamorphic grade (*e.g.,* Schiffman and Liou, 1980); whereas aluminous varieties are restricted to the pumpellyite-actinolite and even to the blueschist-facies zones. Moreover, the effective compositions of precursor minerals seems to be a major factor controlling pumpellyite composition. According to the Al:Fe:Mg projection (Fig. 4a), pumpellyites from the Jurassic rocks studied plot in the prehnite-pumpellyite facies field (straddling the Jonestown and Vancouver island reference fields). The occurrence of pumpellyite types (with different Al_2O_3 content; Table 2b, Fig. 4b) in the same sample is (probably) best interpreted in terms of evolving fO_2 conditions. In fact, variations in the Al $\Leftrightarrow Fe^{3+}$ content in pumpellyite is typical, not only at a same sample level, but also inside a same crystal.

The hydrogarnet-pumpellyite-chlorite-epidote (± prehnite) assemblage may form during the burial induced metamorphism of basic rocks in prehnite-pumpellyite facies (Coombs *et al.*, 1977; Morata *et al.*, 2003) or even in the upper zeolite facies (Aguirre 1992). Coombs *et al.* (1977) state that grandite-chlorite assemblages are common in metabasites of very low metamorphic grade, but are eliminated before the onset of greenschist facies conditions because grandite is incompatible with chlorite in the presence of quartz under such conditions. Therefore, the mineral assemblage hydrogarnet-pumpellyite-chlorite-epidote (+qz) in sample H7-06 indicates (higher) zeolite to lower greenschist facies conditions, which correlate with the observed KI, b_o and coal rank data of metapelites from Belmar *et al.* (2002).

'Chlorite thermometry' in very low-grade metamorphic rocks (Cathelineau, 1988) has been reviewed by De Caritat *et al.* (1993) and Merriman and Peacor (1999). Although its usefulness has been questioned (Essene and Peacor, 1995; Shau *et al.*, 1990; Jiang *et al.*, 1994; Schmidt *et al.*, 1999), the 'chlorite geothermometer' has been applied to four samples of this study. The andesite H7-06, located east of Hualañé, containing the assemblage chlorite - hydrogarnet - epidote-pumpellyite, yielded a temperature of 237±20°C (n=67); two other volcanic rocks, located ESE of Curepto (H6-2; H6-10; table 2a), containing no diagnostic assemblages, yielded chlorite temperatures of 253±23°C (n =45) and 296±25ºC (n=60). These temperatures are lower than those obtained from experimental data on the stability of hydrogarnet (Liou *et al.*, 1983) which indicate a minimum temperature of *ca.* 340ºC (Fig. 6). On the other hand, according to Rossman and Aines (1991) and Amthauer and Rossman (1998), the water content of hydrogarnet increases with decreasing temperature and/or pressure. In our case, the low (2-4 wt%) H_2O calculated in the hydrogarnet is consistent with this T value.

The inconsistency between calculated chlorite temperatures and those estimated from hydrogarnet stability, as well as the occurrence of zoned pumpellyite and epidote, all indicate non-equilibrium crystallisation conditions.

Middle-Late Jurassic andesite sample H7-06 contains the low-variance assemblage pumpellyite-epidote-chlorite-hydrogarnet-quartz-albite. The thermodynamic data of Berman (1988, 1990), coupled with available solid solution models (Powell

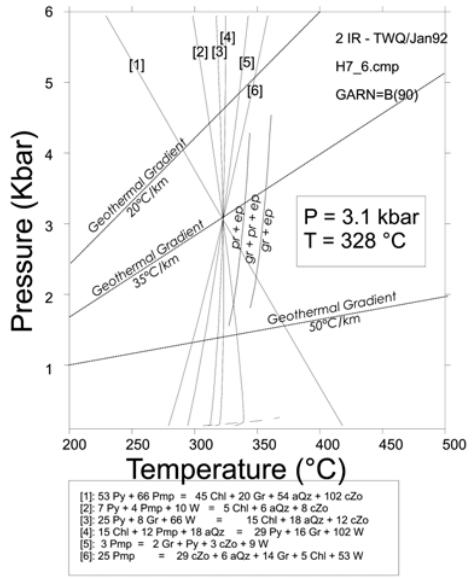

FIG. 6. P-T diagram in the CaO-MgO-Fe_2O_3-Al_2O_3-SiO_2-H_2O (CMFASH) system calculated using the GE0-CALC software (Berman *et al*., 1987). Thermodynamic data base from Berman (1988) including solid-solution model of garnet from Berman (1990). Six multivariant reactions were modelled using pumpellyite (Pmp), hydrogarnet (Py and Gr), chlorite (Chl), epidote (cZo), quartz (aQz) and water (W). Reaction curves for the hydrogarnet (gr), prehnite (pr) and epidote (ep) from Liou *et al.* (1983).

TABLE 2c. TITANITE ANALYSES, CALCULATED ON THE ARBITRARY ASSUMPTIONS 4 Si PER FORMULA UNIT.

	Mean n= 18	St. dev.	Minimum value	Maximum value
SiO_2	30.48	1.56	27.23	34.79
TiO_2	32.12	2.15	28.33	38.41
Al_2O_3	3.18	0.67	2.00	4.82
Fe_2O_3	3.56	1.74	1.41	7.78
MnO	0.12	0.25	0.00	1.10
MgO	0.19	0.44	0.00	1.40
CaO	26.48	1.04	24.35	27.57
Na_2O	0.02	0.01	0.00	0.04
K_2O	0.02	0.01	0.00	0.04
F	0.23	0.11	0.18	0.27
Total	**96.38**	**1.77**	**92.42**	**98.81**
Si	4.00	-	-	-
Ti	3.18	-	-	-
Al	0.49	-	-	-
Fe^{3+}	0.23	-	-	-
Fe^{2+}	0.12	-	-	-
Mn	0.01	-	-	-
Mg	0.04	-	-	-
Ca	3.73	-	-	-
Na	0.00	-	-	-
K	0.00	-	-	-
F	0.02	-	-	-

et al., 1993) and mineral chemistry (Tables 2a, 2b, 2c, 2d), allowed us to locate metamorphic reactions among those minerals on the P-T diagram of figure 6. In the six component system (SiO_2-Al_2O_3-MgO-Fe_2O_3-CaO-H_2O) used in figure 6, there are only 2 independent reactions relating the 7 minerals end members (pyrope, grossular, pumpellyite, clinozoisite, chlorite, quartz and water); therefore the six reactions intersect at the same point at ≈3.1 kbar and ≈328ºC (Fig. 6), implying a dominant geothermal gradient of ≈35ºCkm^{-1} (assuming 3.3. km kbar^{-1}).

SIGNIFICANCE OF THE VLGM

The P-T conditions established for the assemblage pumpellyite-epidote-chlorite-hydrogarnet-quartz-albite in Middle-Late Jurassic lava flows from the Hualañé-Gualleco basin permit the discussion of the geodynamic evolution of the Triassic-Jurassic volcano-sedimentary basins in the Coastal Range of central Chile. Assuming a Carnian-Norian age (≈220 Ma, Geological Time scale of the Geological Society of America, 1999) for the deposition of the Triassic sediments (Corvalán, 1982), a time-interval of *ca*. 40 Ma was obtained by Belmar *et al.* (2004) between deposition and the anchizonal very low-grade metamorphism. According to these authors, an overburden of *ca.* 4.8 km for the anchizonal conditions, corresponding to a high geothermal gradient of >35ºC/km, was calculated. With these figures, the subsidence rate in an extensional geodynamic setting would be of *ca*. 120 m/Ma (Belmar *et al.*, 2004). The geothermal gradient implies that the very low-grade metamorphism could be not only dominated by burial but also controlled by the high regional thermal anomaly related to extension. A zircon fission track age of 206±12 Ma (Willner *et al.*, in press) from Paleozoic granitoids east of the Lago Vichuquén fits the extensional model, with sedimentary basin subsidence, proposed here.

Nevertheless, according to this model, the P-T conditions obtained for the assemblage pumpellyite-epidote-chlorite-hydrogrossular-quartz-albite (≈3 kbar and ≈330ºC, Fig. 6) in Middle-Late Jurassic lavas are not consistent with an evolution of the

TABLE 2d. PUMPELLYITE ANALYSES, BASED ON 16 CATIONS.

Sample	H7-06 Mean n=12	Type 1 St. dev.	Min. value	Max. value	H7-06 Mean n=14	Type 2 St. dev.	Min. value	Max. value
SiO_2	36.68	0.58	35.77	37.40	37.10	0.32	36.69	37.75
Ti_3O_2	0.05	0.06	0.00	0.18	0.05	0.05	0.00	0.16
Al_2O_3	20.70	0.81	19.69	21.64	22.08	0.45	21.24	23.03
FeO	10.12	0.75	9.25	11.75	7.75	0.90	5.56	8.80
MnO	0.10	0.06	0.00	0.20	0.12	0.09	0.02	0.26
MgO	2.10	0.76	1.17	3.98	2.29	0.36	1.82	2.92
CaO	21.72	1.22	19.94	23.55	22.49	0.35	22.01	23.22
Na_2O	0.02	0.02	0.00	0.06	0.02	0.02	0.00	0.05
K_2O	0.02	0.02	0.00	0.08	0.02	0.01	0.00	0.04
Total	**91.49**	**0.77**	**90.29**	**92.88**	**91.89**	**0.70**	**90.60**	**93.14**
Si	6.11	-	-	-	6.10	-	-	-
Ti	0.01	-	-	-	0.01	-	-	-
Al	4.06	-	-	-	4.28	-	-	-
Fe^{2+}	1.41	-	-	-	1.07	-	-	-
Mn	0.01	-	-	-	0.02	-	-	-
Mg	0.52	-	-	-	0.56	-	-	-
Ca	3.87	-	-	-	3.96	-	-	-
Na	0.01	-	-	-	0.01	-	-	-
K	0.00	-	-	-	0.00	-	-	-
XFe	25.77	2.03	23.28	29.06	19.91	2.09	14.63	22.19

TABLE 2e. HYDROGARNET ANALYSES, BASED ON 24 OXYGENS.

Sample	**H7-06 Mean n=32**	**St. dev.**	**Min. value**	**Max. value**
SiO_2	35.72	0.99	34.39	37.71
TiO_2	0.34	0.08	0.18	0.50
Al_2O_3	8.84	0.36	8.25	9.71
Cr_2O_3	0.02	0.03	0.00	0.08
Fe_2O_3	18.33	0.75	17.14	19.74
MnO	0.19	0.06	0.08	0.36
MgO	0.14	0.08	0.00	0.36
CaO	33.16	0.42	32.39	33.86
Na_2O	0.03	0.02	0.00	0.08
K_2O	0.01	0.01	0.00	0.02
V_2O_3	0.41	0.09	0.29	0.54
Total	**96.85**	**1.12**	**94.70**	**99.13**
Si	5.94	-	-	-
Al(IV)	0.09	-	-	-
Al(VI)	1.64	-	-	-
Cr	0.00	-	-	-
Ti	0.04	-	-	-
Fe^{3+}	2.29	-	-	-
V^{3+}	0.05			
Mn	0.02	-	-	-
Mg	0.03	-	-	-
Ca	5.91	-	-	-
Na	0.01	-	-	-
K	0.00	-	-	-
XFe^{3+}	56.95	1.54	53.34	59.41
Grs (%)	42.58	-	-	-
Adr (%)	57.36	-	-	-

All Fe assumed to be Fe^{3+}.

Triassic-Jurassic basins only controlled by subsidence. K-Ar ages available for this area (Belmar *et al.*, 2004) date the diagenesis of sediments at 206 Ma and the anchizone at 184-181 Ma. K-Ar ages of dioritic intrusions range from 165±5 to 175±5 Ma. P-T conditions of the hornfels facies assemblage (ferrosilite-magnesiohornblende-ferroactinolite, biotite together with chlorite, plagioclase and stilpnomelane) in Triassic metapelites range from 655°C to 691°C with pressure <4 kbar (Belmar *et al.*, 2002). Then, assuming a post-Toarcian age (Middle-Late Jurassic, <180 Ma, Geological Time Scale of the Geological Society of America, 1999) for andesitic lavas (as previously indicated), genesis of the assemblage pumpellyite-epidote-chlorite-hydrogarnet-quartz-albite, restricted to these rocks, could not be related with the episode during which maximal anchizonal burial metamorphism (184-181 Ma) was achieved on older Triassic metapelites.

Pumpellyite is a typical metamorphic mineral generated in burial and regional metamorphism. Moreover, the metamorphic assemblage observed in Jurassic lavas is typical of very low-grade metamorphism, excluding the possibility for this assemblage to be a consequence of thermal metamorphism due to the dioritic intrusions.

Therefore the mechanism proposed to explain the genesis of these very low-grade assemblages must be related with another metamorphic event, younger than the burial metamorphism responsible for anchizonal conditions in Triassic metapelites. A change from an extensional (latest Triassic - Middle Jurassic) to compressional (Kimmeridgian-Tithonian) regime has been proposed by Charrier and Muñoz (1994) for the central Chilean Andes. Over this geodynamic setting, and based in the authors' P-T calculations, the authors propose an overthrusting of the Triassic and Lower Jurassic sequences which could favour the increase in lithostatic pressure giving the P-T conditions necessary for the metamorphism in the prehnite-pumpellyite facies.

Hence, two types of very low-grade metamorphism can be differentiated in the studied area. The first one was related with burial, thermally induced, achieving maximal metamorphic conditions of anchizone in Triassic-Jurassic metapelites and dated at 184-181 Ma (Belmar *et al.*, 2002, 2004). A second metamorphic event is observed in Middle to Late Jurassic lavas, with P-T conditions of ≈3 kbar and ≈330ºC, inferred to have been related to overthrusting and crustal thickening following a change from an extensional to a compressional regime.

CONCLUSIONS

In the Triassic-Jurassic basins of the Coastal Range of central Chile (34°45'/35°20'S) sedimentary and intercalated volcanic sequences, restricted to the Middle-Late Jurassic, display evidence of mineralogical re-crystallisation under very low-grade metamorphic conditions. Crystallographic parameters measured in Triassic and Lower Jurassic metapelites (IC and b_0), together with coal and fluid inclusion data are consistent with anchizonal conditions under a ≈ 35°Ckm-1 thermal gradient in an extensional setting, developed during 181-184 Ma (Belmar *et al.*, 2002, 2004). Nevertheless, metamorphic minerals found in stratigraphically younger Middle-Late Jurassic volcanic rocks are consistent with a very low-grade metamorphism developed under prehnite-pumpellyite facies. Pumpellyite composition, chlorite thermometry and P-T calculations indicate P ≈3 kbar ant T ≈300 °C. These P-T conditions are inconsistent with a simple model for metamorphism dominated by burial. Local overthrusting of the Triassic-Lower Jurassic sequences as consequence of a geodynamical change from extensional to compressional regime is proposed in order to re-equilibrate Middle and Late Jurassic volcanic rocks under the estimated P-T conditions.

ACKNOWLEDGEMENTS

This work was benefited by the post-doc MECESUP Grant Nr. 0010. Comments of an early draft by Dr. M. Polvé (Université Paul Sabatier, France) are acknowledged. Critical revisions, comments and suggestions by Dr. L. Aguirre (Universidad de Chile), Dr J. Munhá (Universidade de Lisboa, Portugal) and Dr. A. Willner (Ruhr Universität-Bochum, Germany) improved the original manuscript. The authors thank the University of Basel (Switzerland), for the microprobe and SEM facilities.

REFERENCES

Aguirre, L. 1992. Metamorphic pattern of the Cretaceous Celica Formation, SW Ecuador, and its geodynamic implications. *Tectonophysics* **205**: 223-237.

Aguirre, L.; Féraud, G.; Morata, D.; Vergara, M.; Robinson, D. 1999. Time interval between volcanism and burial metamorphism and rate of basin subsidence in a Cretaceous Andean extension setting. *Tectonophysics* **313**: 433-447.

Aguirre, L.; Levi, B.; Offler, R. 1978. Unconformities as mineralogical breaks in the burial metamorphism of the Andes. *Contributions to Mineralogy and Petrology* **66**: 361-366.

Aguirre, L.; Robinson, D.; Bevins, R.E.; Fonseca, E.; Vergara, M.; Carrasco, J.; Morata, D. 1997. The Valle Nevado stratified sequence: chemistry and alteration pattern. *In Congreso Geológico Chileno, No. 8, Actas* **2**: 1195-1199. Antofagasta.

Aguirre, L.; Robinson, D.; Bevins, R.E.; Morata, D.; Vergara, M.; Fonseca, E.; Carrasco, J. 2000. A low-grade metamorphic model for the Miocene volcanic sequences in the Andes of central Chile. *New Zealand Journal of Geology and Geophysics* **43**: 83-93.

Amthauer, G.; Rossman, G.R. 1998. The hydrous component in andradite garnet. *American Mineralogist* **83**: 835-840.

Beiersdorfer, R.E.; Day, H.W. 1995. Mineral paragenesis in pumpellyite low-grade mafic rocks. *Geological Society of America*, Special Paper **296**: 5-27.

Belmar, M.; Schmidt, S.T.; Frey, M.; Ferreiro-Mählmann, R.; Mullis, J.; Stern, W. 2002. Diagenesis, Low-Grade and Contact Metamorphism in the Triassic-Jurassic of the Vichuquén-Tilicura and Hualañé-Gualleco Basins, Coast Range of Chile. *Schweizeriche Mineralogische und Petrographische Mitteilungen* **82**: 375-392.

Belmar, M.; Morata, D.; Munizaga, F.; Pérez de Arce, C.; Morales, S.; Carrillo, F.J. 2004. Significance of K- Ar dating of very low-grade metamorphism in Triassic-Jurassic pelites from the Coastal Range of central Chile. *Clay Minerals* **39** (2): 151-162.

Berman, R.G. 1988. Internally-consistent thermodynamic data for minerals in the system Na_2O-K_2O-CaO-MgO-FeO-Fe_2O_3-Al_2O_3-SiO_2-TiO_2-H_2O-CO_2. *Journal of Petrology* **29**: 445-522.

Berman, R.G. 1990. Mixing properties of Ca-Mg-Fe-Mn garnets. *American Mineralogist* **75**: 328-344.

Berman, R.G.; Brown, T.H.; Perkins, E.H. 1987. GE0-CALC: software for calculation and display of pressure-temperature-composition phase diagrams. *American Mineralogist* **72**: 861-862.

Bettison, L.A.; Schiffman, P. 1988. Compositional and structural variations of phyllosilicates from the Point Sal ophiolite, California. *American Mineralogist* **73**: 62-76.

Bevins, R.E.; White, S.C.; Robinson, D. 1996. The South Wales coalfield: low-grade metamorphis in a foreland basin setting? *Geological Magazine* **133**: 739-749.

Bevins, R.E.; Robinson, D.; Aguirre, L.; Vergara, M. 2003. Episodic burial metamorphism in the Andes - A viable model ?. *Geology* **31**: 705-708.

Bravo, P. 2001. Geología del Borde Oriental de la cordillera de la costa entre los Ríos Mataquito y Maule, VII región. Memoria de Titulo (Inédito), *Universidad de Chile, Departamento de Geología*: 113 p.

Cathelineau, M. 1988. Cation site occupancy in chlorites and illites as a function of temperature. *Clay Minerals* **23**: 471-485.

Charrier, R.; Muñoz, N. 1994. Jurassic Cretaceous palaeogeographic evolution of the Chilean Andes at 23°-24° latitude and 34°-35° latitude: a comparative analysis. *In* Tectonics of the Southern Central Andes. Structure and evolution of an active continental margin (Reutter, K.J.; Scheuber, E.; Wigger, P.J.; editors). *Springer-Verlag*: 233-242.

Coombs, D.S.; Nakamura, Y.; Vuagnat, M. 1976. Pumpellyite-actinolite facies schists of the Taveyanne Formation near Loèche, Valais, Switzerland. *Journal of Petrology* **17**: 440-471.

Coombs, D.S.; Kawachi, Y.; Houghton, B.F.; Hyden, G.; Pringle, I.J.; Williams, J.G. 1977. Andradite and andradite-grossular solid solutions in very low-grade regionally metamorphosed rocks in Southern New

Zealand. *Contributions to Mineralogy and Petrology* **63**: 229-246.

Corvalán J. 1982. El Límite Triásico-Jurásico en la Cordillera de la Costa de las Provincias de Curicó y Talca. *In Congreso Geológico Chileno, No. 3, Actas* **3:** F63-F-85. Concepción.

De Caritat, P.; Hutcheon, I.; Walshe, J.L. 1993. Chlorite geothermometry: a review. *Clays and Clay Minerals* **41**: 219-239.

England, T.D.E.; Bustin, R.M. 1985. Effect of thrust faulting on organic maturation in the Southeastern Canadian Cordillera. *In A*dvances in Organic Geochemistry 1985 (Leythäuser, D.; Rullkötter, J.; editors). *Pergamon***:** 609-616.

Essene, E.J.; Peacor, D.R. 1995. Clay mineral thermometry- a critical perspective. *Clays and Clay Minerals* **43**: 540-553.

Ferreiro Mählmann, R. 2001. Correlation of very low grade data to calibrate a thermal maturity model in a nappe tectonic setting, a case study from the Alps. *Tectonophysics* **334**: 1-33.

Frey, M.; Robinson, D. (Editors). 1999. Low-grade metamorphism. *Blackwell Science Ltd*.: 313 p.

Frey, M.; de Capitani, C.; Liou, J.G. 1991. A new petrogenetic grid for low-grade metabasites. *Journal of Metamorphic Geology* **9**: 497-509.

Gana, P.; Hervé, F. 1983. Geología del basamento cristalino en la Cordillera de la Costa entre los ríos Mataquito y Maule, VII Región. Chile. *Revista Geológica de Chile* **19 (**20): 37-56.

González-Bonorino, F.; Aguirre, L. 1970. Metamorphic facies series of the crystalline basement of Chile. *Geologische Rundschau* **59**: 979-994.

Guidotti, C.V.; Sassi, F.P. 1986. Classification and correlation of metamorphic facies series by means of muscovite b_0 data from low-grade metapelites. *Neus Jahrbuch für Geologie und Palaontologie, Abhandlungen* **153**: 363-380.

Hervé, F. 1988. Late Paleozoic Subduction and Accretion in Southern Chile. *Episodes* **11**: 183-188.

Hervé, F.; Kawashita, K.; Munizaga, F. 1982. Edades Rb/Sr de los cinturones metamórficos pareados de Chile central. *In Congreso Geológico Chileno, No. 3, Actas* **2:** d116-d135. Concepción.

Hunziker, J.C.; Frey, M.; Clauer, N.; Dallmeyer, R.D.; Friedrichsen, H.; Flehmig, W.; Hochstrasser, K.; Roggwiler, P.; Schwander, H. 1986. The evolution of illite to muscovite: mineralogical and isotopic date from the Glarus Alps Switzerland. *Contributions to Mineralogy and Petrology* **92**: 157-180.

Jiang, W.T.; Peacor, D.R.; Buseck, P.R. 1994. Chlorite geothermometry?-contamination and apparent octahedral vacancies. *Clays and Clay Minerals* **42**: 593-605.

Kübler, B. 1967. La crytallinité de i'illite et les zones tout à fait supérieures du métamorphisme. *Colloques Étages tectoniques', Neuchâtel*: 105-122.

Kübler, B. 1984. Les indicateurs des transformations physiques et chimiques dans la diagenèse, température et calorimétrie. *In* Thérmométrie et barométrie géologiques (Lagache, M.; editor). *Societé Française de Minéralogie et Cristallographie*: 489-596. Paris.

Langenberg, W.; Kalkreuth, W. 1991. Tectonic controls on regional coalification and vitrinite-reflectance anisotropy of Lower Cretaceous coals in the Alberta foothills. *Bulletin de la Societé Géologique de la France* **162** (2): 375-383.

Levi, B. 1969. Burial metamorphism of a Cretaceous volcanic sequence West from Santiago, Chile. *Contributions to Mineralogy and Petrology* **24**: 30-49.

Levi, B.; Aguirre, L.; Nyström, J.O. 1982. Metamorphic gradients in burial metamorphosed vesicular lavas: comparison of basalt and spilite in Cretaceous basic flows from central Chile. *Contributions to Mineralogy and Petrology* **80**: 49-58.

Liou, J.G.; Ernst, W.G. 1979. Oceanic ridge metamorphism of the East Taiwan Ophiolite. *Contributions to Mineralogy and Petrology* **68**: 335-342.

Liou, J.G.; Kim, H.S.; Maruyama, S. 1983. Prehnite-epidote equilibria and their petrologic applications. *Journal of Petrology* **24**: 321-342.

Martin, M.W.; Kato, T.T.; Rodríguez, C.; Godoy, E.; Duhart, P.; McDonough, M.; Campos, A. 1999. Evolution of the late Paleozoic accretionary complex and overlying forearc-magmatic arc, south central Chile (38º-41ºS): constraints for the tectonic setting along the southwestern margin of Gondwana. *Tectonics* **18**: 582-605.

Merriman, R.J.; Frey, M. 1999. Patterns of very low-grade metamorphism in metapelitic rocks. *In* Low-grade metamorphism (Frey, M.; Robinson, D.; editors). *Blackwell Science Ltd*.: 61-107.

Merriman, R.J.; Peacor, D.R. 1999. Very low-grade metapelites: mineralogy, microfabrics and measuring reaction progress. *In* Low-grade metamorphism (Frey, M.; Robinson, D.; editors). *Blackwell Science Ltd*.: 10-60.

Morata, D.; Aguirre, L.; Belmar, M.; Morales, S. 2003. Constraining very low-grade metamorphic conditions based on prehnite chemistry. *In Congreso Geológico Chileno,No. 10*, *Actas*, CD Rom. Concepción.

Morel, R. 1981. Geología del sector norte de la hoja Gualleco, entre los 35°00' y los 35°10' latitud sur, provincia de Talca, VII región, Chile. Tesis de grado, Master in Sciences (Inédito), *Universidad de Chile, Departamento de Geología*: 149 p.

Munizaga, F.; Aguirre, L.; Hervé, F. 1973. Rb/Sr ages of rocks from the Chilean metamorphic basement. *Earth and Planetary Science Letters* **18**: 87-91.

Nyström, O.J. 1983. Pumpellyite-bearing rocks in Central Sweden and extent of host rock alteration as a control of pumpellyite composition. *Contributions to Mineralogy and Petrology* **83**: 159-168.

Powell, W.G.; Carmichael, D.M. ; Hodgson, C.J. 1993. Thermobarometry in a subgreenschist to greenschist transition in metabasites of the Abitibi greenstone

belt, Superior Province, Canada. *Journal of Metamorphic Geology* **11**: 165-178.

Robinson, D.; Bevins, R.E.; Rowbotham, G. 1993. The characterization of mafic phyllosilicates in low-grade metabasalts from eastern North Greenland. *American Mineralogist* **78**: 377-390.

Robinson, D.; Bevins, R.E.; Aguirre, L.; Vergara, M. 2004. A reappraisal of episodic burial metamorphism in the Andes of central Chile. *Contributions to Mineralogy and Petrology* **146**: 513-528.

Rossman, G.R.; Aines, R.D. 1991. The hydrous components in garnets: grossular-hydrogrossular. *American Mineralogist* **76**: 1153-1164.

Ruiz-Cruz, M.D.; Puga, E.; Aguirre, L.; Vergara, M.; Morata, D. 2002. Vermiculite-like minerals in low-grade metasediments from the Coastal Range of central Chile. *Clay Minerals* **37:** 221-234.

Ruiz-Cruz, M.D.; Morata, D.; Puga, E.; Aguirre, L.; Vergara, M. (2004). Microestructures and interlayering in pyrophilite from the Coastal Range of central Chile: evidence of disequilibrium assemblage. *Clay Minerals*: **39**: 439-452.

Sassi, F. P.; Scolari, A. 1974. The b_o value of the potassium white micas as a barometric indicator in low-grade metamorphism of pelitic schists. *Contributions to Mineralogy and Petrology* **45**: 143-152.

Schiffman, P.; Fridleifsson, G.O. 1991. The smectite-chlorite transition in drill-hole NJ-15, Nesjavellir geothermal field, Iceland: XRD, BSE and electron microprobe investigations. *Journal of Metamorphic Geology*: **9**: 679-696.

Schiffman, P.; Liou, J.G. 1980. Synthesis of Fe-pumpellyite and its stability relations with epidote. *Journal of Metamorphic Geology* **1**: 91-101.

Schmidt, D.; Livi, K.J.T.; Frey, M. 1999. Reaction progress in chloritic material: an electron microbeam study of the Taveyanne greywacke, Switzerland. *Journal of Metamorphic Geology* **17**: 229-241.

Schmid, D.; Schmid, S.T.; Mullis, J.; Ferreiro-Mählmann, R.; Frey, M. 1997. Very low-grade metamorphism of the Taveyanne formation of Western Switzerland. *Contributions to Mineralogy and Petrology* **129**: 385-403.

Shau, Y.H.; Peacor, D.R.; Essene, E. J. 1990. Corrensite and mixed-layer chlorite/corrensite in metabasalt from Northern Taiwan: TEM/AEM, EMPA, XRD, and optical studies. *Contribution to Mineralogy and Petrology* **105**: 123-142.

Thiele, R.; Morel, R. 1981. Tectónica triásico-jurásica en la Cordillera de la Costa, al norte y sur del río Mataquito (34° 45' - 35° 15' lat. s), Chile. *Revista Geológica de Chile* **13** (14): 49-61.

Vergara, M.; Levi, B.; Villaroel, R. 1993. Geothermal-type alteration in a burial metamorphosed volcanic pile, central Chile. *Journal of Metamorphic Geology* **11**: 449-454.

Willner, A.P.; Thomson, S.N.; Kröner, A.; Wartho, J.A.; Wijbrans, J.; Hervé, F. (In press). Time markers for the evolution and exhumation history of an Upper Paleozoic paired metamorphic belt in Central Chile (34°-35°30´S). *Journal of Petrology*.

Willner, A.P.; Hervé, F.; Massonne, H.-J. 2000. Mineral chemistry and pressure-temperature evolution of two contrasting high-pressure-low-temperature belts in the Chonos Archipelago, Southern Chile. *Journal of Petrology* **41**: 309-330.

Manuscript received: September 1, 2004; accepted: May 13, 2005.